


Simple Mechanism for Optimal Light-Use Efficiency of Photosynthesis Inspired by Giant Clams

Amanda L. Holt 


Department of Physics, Yale University, New Haven, Connecticut 06511, USA

Lincoln F. Rehm 

*Department of Biodiversity, Earth and Environmental Science, Drexel University, Philadelphia, Pennsylvania 19104, USA
and Palau International Coral Reef Center, Koror, Palau*

Alison M. Sweeney*

Departments of Physics and Ecology & Evolutionary Biology, Yale University, New Haven, Connecticut 06511, USA

 (Received 13 June 2023; revised 1 May 2024; accepted 6 May 2024; published 28 June 2024)

In photosymbiotic giant clams, vertical columns of single-celled algae absorb sunlight that has first been forward scattered from a superficial layer of light-scattering cells called iridocytes. In principle, this arrangement could lead to a highly efficient system but it has been unclear how to calculate a productivity denominator to normalize the performance of the system. Inspired by the geometry observed in the clam, we have created an analytical model that calculates the idealized performance of a system with a geometry similar to the clam. In our model, photosynthesis-irradiance behavior obeys that of algal cells isolated from clams. Using a standard rate of eight photons of photosynthetically active radiation required to create one molecule of O₂, we find that a fixed geometry of the “light-dilution” strategy employed by the clams can reach a quantum efficiency of 43% relative to the solar resource in intense tropical sunlight. In comparing the performance of the model to published photosynthesis-irradiance relations of living clams, we have observed that the living system easily exceeds the performance of the static model. Therefore, we have next considered a model in which the system geometry changes dynamically to optimize the quantum efficiency as a function of the solar irradiance. In this scenario, with changes in irradiance typical of a sunny tropical day, the performance of the model was consistent with that of large mature living clams and had a quantum efficiency of 67%. We also show that a similar dynamic modulation of the clam-tissue geometry could plausibly occur in the living animals. We have considered the possibility that efficiency gains in the living system could also occur via further optimization of per-cell absorbance of multiply scattered light within the highly absorbing system. However, a numerical model of radiative transfer within clam tissue that captures realistic multiple scattering has not located efficiency gains relative to the simpler single-pass analytical model. Therefore, we infer that additional resource efficiency over the dynamic, large-clam-like model would require nontrivial organization among cells at small length scales. We also observe that boreal spruce forests coupled to atmospheric haze may realize the same scale-invariant scattering-and-absorbance strategy as the clams but at a different, larger, length scale. Given these results, our model may demonstrate the maximum realizable light-use efficiency of a large photosynthetic system relative to the solar resource. The general principles here also readily generalize to any photosynthetic cell type or organic photoconversion material and solar-irradiance regime. They could therefore provide inspiration both for engineering novel efficient photoconversion processes and materials and inform optimal land-use estimates for efficient industrial biomass production.

DOI: [10.1103/PRXEnergy.3.023014](https://doi.org/10.1103/PRXEnergy.3.023014)

*Corresponding author: alison.sweeney@yale.edu

Published by the American Physical Society under the terms of the [Creative Commons Attribution 4.0 International](https://creativecommons.org/licenses/by/4.0/) license. Further distribution of this work must maintain attribution to the author(s) and the published article's title, journal citation, and DOI.

I. INTRODUCTION

What is the maximum possible efficiency and productivity of a large-scale photosynthetic system? Photosynthesis contains an energy-efficiency paradox. At large spatial and temporal scales, photosynthetic ecosystems are surprisingly inefficient at utilizing the solar resource. Crops grown under high solar irradiance for food and fuel only convert around 3% of the energy in sunlight into usable photosynthate (see, e.g., Ref. [1]). In contrast, at small length and time scales, the photosystems that perform the initial electron-separation event converting light energy into chemical energy approach 100% efficiency [2]. As a simple matter of energy conservation, the light reactions of photosynthesis require eight photons of photosynthetically active radiation to fix one molecule of O_2 [3]. In crops growing in soil, there is probably no straightforward way for the high potential resource efficiency of the light reactions to transmit to production of biomass [1]. Unicellular algae, as they do not require roots, shoots, or complex vasculature to connect the two, have the potential to be especially resource efficient both in the photosynthetic light reactions and in the movement of energy from the light reactions to carbon fixation.

The modern economy runs on photosynthetic products accumulated over geologic time. Cultivation of unicellular algae at the industrial scale is a potential route to economically meaningful quantities of nonfossil liquid fuels and chemical feedstocks. This is because algae can be grown at high densities in liquid culture and many species readily deposit a majority of photosynthesized carbon into intracellular oil droplets rather than in complex extracellular polymers [4]. The field presently employs many geometric strategies for large-scale liquid-cultivation schemes such as open ponds, cylindrical tubes, spherical bags, falling droplets, and internal illumination [5,6]. These strategies all have an optical path length that is large compared to the mean free path between cells in the dense culture, such that Beers law and exponential decay govern the radiative transfer through the system [7]. Because the light-use efficiencies of single cells are strongly dependent on the light intensity, an exponential decay of light through a dense culture means that a few cells experience too high a light intensity to be efficient and many cells experience too low a light intensity to be highly productive [8]. Various architectures using internal artificial illumination can lead to greater per-cell and system productivity but suffer critically from higher monetary and energy-input costs relative to using ambient sunlight as the energy source [9,10].

To address the question of just how light efficient any area-spanning system for algal cultivation under ambient sunlight can be, we consider the case of the giant clam (genus *Tridacna*). These animals are symbiotic with unicellular algae in the dinoflagellate genus *Symbiodinium*. In this symbiosis, the algae live in the mantle tissue,

performing photosynthesis and contributing energy to the host in the form of small organic molecules. The large clam uses its large filter-feeding apparatus to contribute nitrogen and other nutrients to the system [11,12]. Through a reanalysis of experimental data from a classic 1985 paper [11], we demonstrate here that at tropical solar intensities, large clams photosynthesize at rates that reflect near-perfect efficiency in the initial oxygen-evolution step of photosynthesis. Here, we develop a simple physical model of light scattering and photoconversion that can explain how this unprecedented efficiency is likely achieved in the clam system.

Giant clams are a group of photosymbiotic bivalves with around a dozen species in the genus *Tridacna*. They live in shallow coral-reef environments throughout the tropical Indo-Pacific oceans. The animals are free spawning and larvae develop in the water column and begin feeding on phytoplankton. The ingestion of algal cells lead to the larvae settling on to a coral reef and developing into a small clam with photosynthetic algae in its mantle tissue. As the clam grows, the initial population of unicellular algae multiply and develop into an array of vertical columnar structures in the mantle tissue of the clam [13]. These algal columns are roughly $100\ \mu\text{m}$ in diameter and approximately $150\ \mu\text{m}$ apart. In contrast, very similar unicellular algae exist as photosymbionts in coral tissues, where they are diffusely organized in a monolayer. This difference in the geometry of the organization of the algae in the tissue is easily visible by eye: where algae are visible in the clam tissue beneath and around the superficial iridocytes, the mantle tissue appears saturated black [Fig. 1(a)]. In contrast, reef-building corals

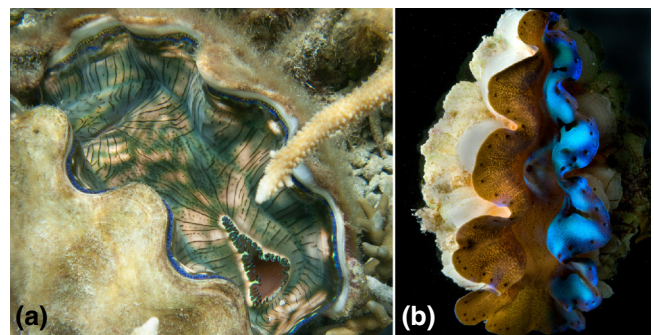


FIG. 1. (a) A giant clam on a Palauan coral reef adjacent to reef-building corals in the genus *Acropora*. Both species harbor photosymbionts in the genus *Symbiodinium* but the overall reflectance of the two animals is quite different. (b) A small individual *T. crocea*, with strong directional illumination from the left. Under this asymmetric illumination, the forward-scattering iridocytes on the left side of the animal become transparent, revealing regular arrays of algae organized into an array of vertically oriented cylinders.

are generally a paler biscuitlike color due to the less-dense packing of algae in the tissue [Fig. 1(a)]. When the clams are under strongly directional lateral illumination, the forward-scattering iridocytes become transparent and reveal the columnar arrays of densely packed microalgae within the mantle tissue that lead to the appearance of saturated black mantle tissue under overhead illumination [Fig. 1(b)].

Given the differences in density and organization of photosymbionts between clams and corals, it is interesting to consider the performance of clams in comparison to corals and with respect to the solar resource. When *in hospite* with a coral, *Symbiodinium* are very efficient at the scale of individual cells, approaching theoretical limits [14]. In low light, at mesophotic depths of 40–50 m, corals can be highly solar-resource efficient [15]. However, considered at the scale of the whole organism and the solar resource in shallow water and high irradiances, the coral system is quite inefficient, since only around 80% of available sunlight is absorbed and 96% of that absorbed light is dissipated as heat [14,16].

Unlike corals, giant clams are not known to live at mesophotic depths. Where we have worked with giant clams in Palau (where the photographs in Fig. 1 were taken), the animals are commonly found in reef locations that are exposed at low tide and are only infrequently found at depths greater than 10 m. Palau is located at 7°N latitude and for much of the year the weather is clear, such that these low-tide-exposed clams regularly experience some of the most intense sunlight on Earth. A weather station located at Palau International Coral Research Center (PICRC) in Koror, Palau, where our prior experimental work on these animals took place, shows that a typical midday irradiance at ground level can be $1500 \mu\text{E m}^{-2} \text{s}^{-1}$ [17]. The effects of wave-lensed caustics in these very clear and shallow waters can amplify the average background irradiance by tenfold for brief pulses [18], such that considering a time-averaged background irradiance may even underestimate the irradiances experienced over short time scales by the clam system. Because clams have more, and more densely packed, algae than corals immediately adjacent to them on the same reefs and are also absorbing some of the most intense sunlight on Earth, they seem a particularly interesting system to investigate solar-resource efficiency in intense natural sunlight.

The clam mantle tissue contains iridocytes, light-scattering cells the optical behavior of which we have previously described [19,20]. Iridocytes contain dense approximately 100-nm-thick platelets organized orthogonal to the direction of incoming light layered within a round cell of approximately 8 μm diameter. These cells scatter collimated downwelling sunlight forward into the tissue of the clam in a cone about 15° wide. (It is reasonable to consider light entering the clam to be collimated

due to the phenomenon of Snell's window refracting light into the water at a fixed near-downwelling angle at the air-water interface.) The algae in the clam mantle tissue are positioned under the iridocytes. These algae are about 10 μm in diameter and loosely packed into vertical columns that are roughly 100 μm in diameter and 150 μm apart. Due to the scattering of the iridocytes, the surfaces of these columns experience a roughly equal light intensity along the entire length [19]. The system can be conceptualized as a solar transformer, in which a high incident solar flux is down-converted via light scattering from the iridocytes, resulting in a lower local flux over a larger area at the surfaces of the pillars. Our previous work suggests that the individual algae in the system experience local light intensities that are roughly 10% of the initial intensity incident on the surface of the system, and almost all of the light incident on the system is absorbed at the lower local flux [19]. We do not currently understand the actual or possible resource-scale energy efficiency of such a system, however.

Other prior work on photosynthesis in giant clams has been conducted from an organismal-physiology perspective and has focused on the extent to which the clam meets its metabolic needs through photosynthesis of the symbionts versus filtering particles using the gills of the animal (see, e.g., Refs. [11,21–23]). In this prior physiological context, it has been determined that larger clams both meet more of their carbon requirement from photosynthesis [24] and are healthy and photosynthetically efficient at relatively high light intensities [21,23]. These results are consistent with the animals having high light-use efficiencies that also increase as the animals grow but these studies do not directly address the question of how efficiently any given clam converts the solar resource to chemical energy.

Because the efficiency of biological photosynthesis generally increases with decreasing flux [25], the solar-transformer geometry of the clam suggests that such an arrangement could also be highly efficient at solar energy conversion. The objective of this work is to develop a simple framework for understanding what large-scale resource-level efficiencies are physically plausible for photosynthesis in such a solar-transformer design. What is the overall performance of the system and does it allow the symbiosis to approach anything like a perfectly efficient use of the solar resource using natural photosynthesis?

We have developed a simple physical model to understand how the evolved tissue structure of the clam relates to the optimization of solar-resource efficiency. We model the clam system as a simple vertically oriented cylinder in which light incident on the horizontal circular top surface (analogous to the iridocytes) is uniformly redistributed along the inner vertical wall (analogous to a radially averaged set of nearest-neighbor columns of algae) (Fig. 2, bottom right). The walls of the cylinder perform with the

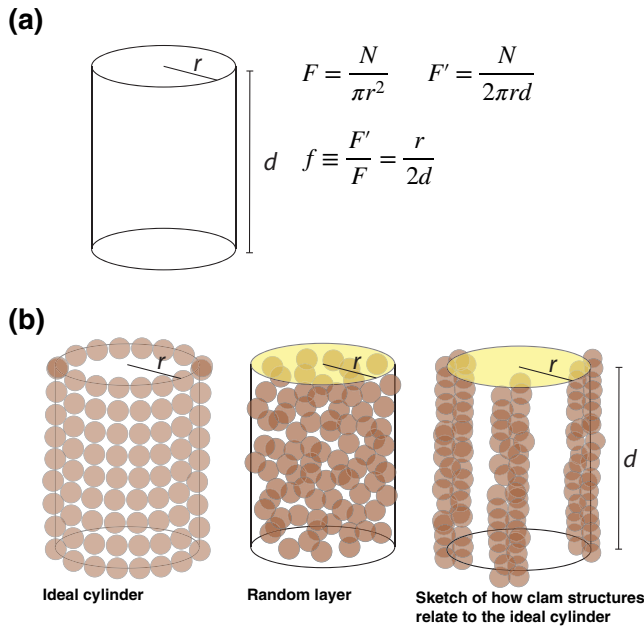


FIG. 2. A schematic of the simple-cylinder model. (a) The model geometry and parameters. (b) The schematic arrangement of cells in (left to right) the “ideal-cylinder” case and the “random-layer” case and how the more literal clam-tissue geometry containing columns of algae compares to these geometrically simpler cases.

photosynthesis-irradiance behavior of a dilute suspension of algae that were isolated from a giant clam in prior work ([11], Fig. 2). We can then consider analytically the interplay of system geometry and efficiency.

We use this simplification to explore the resource efficiency using the parameters of rate of O_2 evolution per area, as a function of irradiance and as a function of solar irradiance considered over a day. We then compare the performance of this simple cylindrical system to one with the same physical size and total number of algal cells but with the algae uniformly and randomly arranged throughout the volume.

Then, to explore the effects of multiple scattering that occur in the more geometrically complicated system of columns of algae in the real clam, we compare this simple analytical model to a numerical model of light scattering of a more realistic system with discrete realistic cell positions and the actual geometry of the clam system.

We find that if the geometry of the simple-cylinder system can be modulated with light intensity via cycles of inflation and deflation of the mantle tissue, leading to expansion and contraction of the effective cylinder radius with light intensity, the model approaches 70% quantum efficiency with respect to the solar resource over a realistic day of solar flux in the tropics. Inflation and deflation of the mantle tissue is a major part of the behavior of a clam, observed most typically in a “flinching” response to perturbation. In this scenario, the mantle should be

relatively deflated in high light, decreasing the effective radial spacing between columns, thereby increasing the factor by which light is diluted and decreasing our parameter f . In low light, the mantle should inflate, increasing the effective radial column spacing, decreasing light dilution, and increasing our parameter f .

Similarly, if the algae within the living clam are also able to position themselves within columns to optimize the per-cell absorbance of “second-pass” radiation inside the columns, it is physically plausible for the clam system to achieve near-perfect solar-resource efficiency, as is suggested to be possible from literature photosynthesis-irradiance data for large living clams (see our re-analysis of [11], below).

II. THEORY

In our simple model of a biological solar transformer, we consider a cylinder. Light incident on the horizontal circular top of the cylinder is redirected through scattering such that the flux on the vertical sides of the cylinder is constant at every point.

The flux on the top of the cylinder in a time interval t is

$$F = \frac{N}{\pi r^2}, \quad (1)$$

where N is a number of photons per time, r is the radius of the cylinder, and F is the incident solar flux (Fig. 2).

We imagine that the horizontal top surface of the cylinder scatters downwelling incident light such that the flux on the vertical wall of the cylinder is equal at every point. In this scenario, the flux on the inside of the cylinder will be

$$F' = \frac{N}{2\pi r d}, \quad (2)$$

where N is the number of photons per time incident on the surface and d is the vertical depth of the cylinder (Figs. 2 and 3).

The photon flux experienced at the walls of the cylinder is then related to the ratio of the area of the circular top of the cylinder to the area of the vertical wall of the cylinder. We define a flux down-conversion factor f dictated by the geometry of the cylinder:

$$f \equiv \frac{F'}{F} = \frac{\frac{N}{2\pi r d}}{\frac{N}{\pi r^2}} = \frac{r}{2d}. \quad (3)$$

We then consider that the vertical wall of the cylinder is uniformly covered in unicellular algae such that the effective number of cells in the system, n , is the surface area of the cylinder divided by the projected area of a single

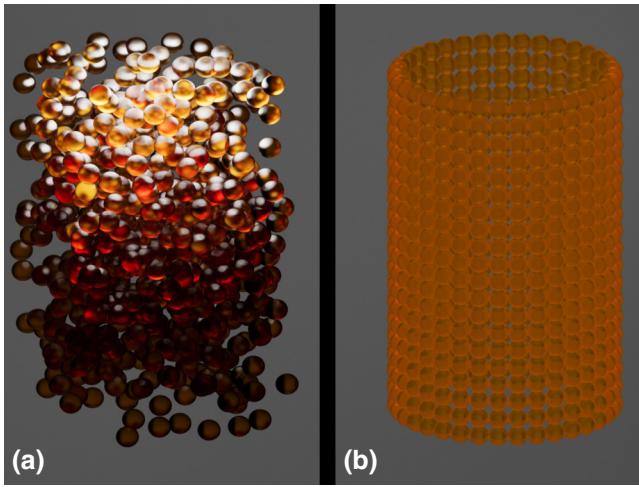


FIG. 3. (a) A conceptual rendering of light propagation through a random layer of *Symbiodinium*. (b) A conceptual rendering of light propagation through a simple model cylinder in which each cell in the wall of the cylinder experiences the same light intensity.

spherical cell with radius R :

$$n = \frac{2\pi rd}{\pi R^2}. \quad (4)$$

To estimate how photosynthesis performs as a function of this geometry, we have used an analytical model of photosynthesis-irradiance behavior developed by Eiler and Peeters [25]. We summarize it here to emphasize the analytical and experimental grounding of the present work. Eiler and Peeters's model captures the essential steady-state features of biological phototransduction using a set of differential equations. Consider that a photosystem can be in one of three states: resting, activated, or inhibited. A resting photosystem absorbs a photon, transitioning to the activated state. The rate α of these transitions will be proportional to the light intensity I . During a short time interval t , the photosystem generates a unit of chemical energy, after which the photosystem returns to the resting state with rate constant γ . However, if the photosystem absorbs a second photon while still in the activated state, it can become inactivated. The mean rate of transition β from the activated to the inactivated state is then also proportional to the intensity. Photoinhibition develops slowly relative to energy production, so β will be smaller than α . Photosystems transition from the inhibited state back to the resting state through a slower repair process with rate δ . The probability of being in the resting state is P_1 , the probability of being in the active state is P_2 , and the probability of being in the inhibited state is P_3 , with $\overline{P_1}$, $\overline{P_2}$, and $\overline{P_3}$ defining the values at steady state. With this simple model, the authors of [25] have derived a set of differential equations that generate a very general and accurate

description of experimentally measured photosynthesis-irradiance behavior of living systems, summarized as follows.

First, a given photosystem must be in one of the three defined states such that

$$P_1 + P_2 + P_3 = 1. \quad (5)$$

Then, the set of possible transitions corresponds to

$$\begin{aligned} \frac{dP_1}{dt} &= -\alpha IP_1 + \gamma P_2 + \delta P_3, \\ \frac{dP_2}{dt} &= \alpha IP_1 - (\beta I + \gamma) P_2, \end{aligned} \quad (6)$$

and

$$\frac{dP_3}{dt} = \beta IP_2 - \delta P_3.$$

The rate of production of the system at steady state, p , for a given intensity I is then

$$p = kN\overline{P_2} = \frac{k\alpha\gamma\delta NI}{\alpha\beta I^2 + (\alpha + \beta)\delta I + \gamma\delta}, \quad (7)$$

where N is the number of photosystems and k is a proportionality constant with units of the rate of photosynthetic production.

By writing

$$a = \frac{\beta}{k\gamma\delta N}, \quad b = \frac{(\alpha + \beta)}{\alpha k\gamma N}, \quad \text{and} \quad c = \frac{1}{k\alpha N}, \quad (8)$$

we can find a simple expression of the rate of production of the system as a function of irradiance to be

$$p = \frac{I}{aI^2 + bI + c}. \quad (9)$$

Eiler and Peeters's parameters a , b , and c are then convenient and theoretically grounded quantities that provide excellent fits to the experimental photosynthesis versus irradiance (PI) behavior of a photosynthetic system [25]. For a unit of light energy, we use the einstein (E), or a mole of photons in the photosynthetically active range of 400–750 nm, so that our units of light flux become $\mu\text{E m}^{-2} \text{s}^{-1}$.

To use this model of photosynthesis in a clamlike geometry, we repurpose experimental data from a study of giant-clam photosynthesis by Fisher and colleagues [11]. Fisher and colleagues have isolated algae from giant-clam mantle tissue and determined photosynthesis-irradiance parameters for a dilute suspension of algal cells to be $a = 1.32 \times 10^{-4}$ [$\mu\text{g chlA h}/\mu\text{mol O}_2(\mu\text{E}/\text{m}^{-2} \text{s}^{-1})$], $b = 2.75$ ($\mu\text{g chlA h}/\mu\text{mol O}_2$), and $c = 122$ [$(\mu\text{E}/\text{m}^{-2} \text{s}^{-1}) \mu\text{g chlA h}/\mu\text{mol O}_2$ (Fig. 4).

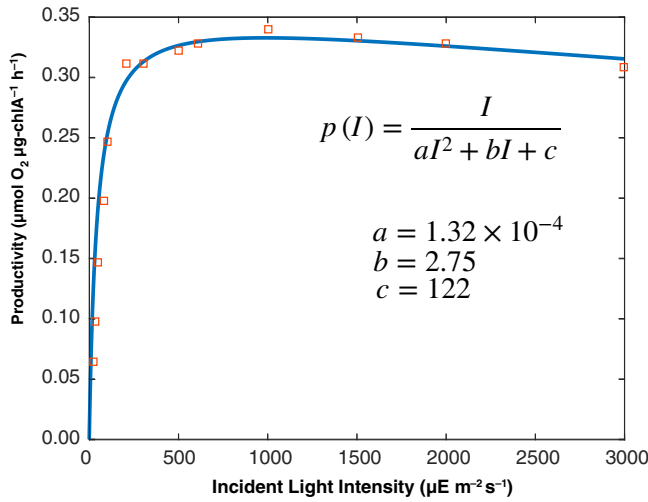


FIG. 4. The photosynthesis-irradiance relation for dilute *Symbiodinium* from Fisher and colleagues [11]. The red squares indicate experimental data points and the blue line indicates the equation fitted to these data.

If a suspension of algal cells is dilute such that all cells in the system experience the same incident flux, the resulting experimental PI relation can be used to calculate the production of dense systems of cells with changing internal irradiance.

In a randomly organized dense layer of algae, radiance decays from the surface exponentially with depth z and attenuation coefficient ε according to Beers law:

$$I(z) = I_0 e^{-\varepsilon z}. \quad (10)$$

The productivity of the dense layer can be found by integrating the photosynthesis-irradiance relation of the dilute system by depth. The integrated rate of production P over a depth of z of a dense layer will be

$$P = \int_0^z p(I(z)) dz. \quad (11)$$

If scattering is minimal, the attenuation coefficient of the system approaches the single-cell absorption coefficient and ε of the random system will be the product of a single-cell absorption cross section and the number density of the system, resulting in units of attenuation per meter. We use a single-cell absorption cross section of $56 \mu\text{m}^2$, estimated from our own measurements and similar to literature values for *Symbiodinium* algae (see, e.g., Ref. [26]).

By combining Eq. (10) with Eq. (11), it is possible to obtain an analytical solution for the integrated productivity of the system over a specified range of light intensities. See Eiler and Peeters for a detailed derivation (see Ref. [25, Eqs. (42)–(45)]).

In contrast, the intensity with depth along the walls of our model cylinders will, by definition, be constant

for a given cylinder geometry and corresponding flux down-conversion factor f [Eq. (3)]:

$$I_{\text{cyl}} = I_0 f. \quad (12)$$

The depth-integrated productivity for the cylinder, as defined in Eq. (11), will be

$$P = p(I_0 f) d. \quad (13)$$

Using the original dimensions of Fisher and colleagues [11], the depth-integrated production has dimensions of $\mu\text{mol O}_2 \text{ m } \mu\text{g}_{\text{chlA}}^{-1} \text{ h}^{-1}$. We can then normalize this result by the mass of chlorophyll A per cell (2.5 pg per cell, also reported in Ref. [11]) to find the areal productivity of the system in $\mu\text{mol O}_2 \text{ m}^{-2} \text{ h}^{-1}$. We can also define a simple metric of light-use efficiency of any of our systems from the energetic requirement of eight photons of absorbed light required to make one molecule of O_2 [3] and we define this relative to the incident flux, not the energy absorbed by the system.

We have used this analytical framework to estimate the system productivity for idealized cylinders with evenly illuminated walls that behave like living *Symbiodinium* cells. We have compared the behavior of these cylinders to layers of the same dimension with the same number of cells organized randomly in the volume. The qualitative visual difference between light attenuation between the two-cylinder versus the random-layer system is shown in Fig. 3.

III. PRODUCTIVITY OF THE SIMPLE MODELS

A. Productivity in the f - I plane

We have calculated the depth-integrated rate of production [Eq. (10)] and the corresponding area-normalized production for a set of cylinders of increasing aspect ratio but small absolute size, the optical behavior of which is described in Eq. (3). We have fixed the radius of the top of the cylinder at a size of $700 \mu\text{m}$, which approximates the nearest-neighbor distance between pillars in the living clam system [19]. We have considered a range of aspect ratios corresponding to f from $f=0.001$ to 1, which results in a range of cylinder depths from 35 cm to $350 \mu\text{m}$. We have calculated the productivity over a range of incident-light intensities from 0 to $3000 \mu\text{E m}^{-2} \text{ s}^{-1}$. We have then compared the performance of these simple idealized cylinders to the depth-integrated productivity rate for a randomly organized layer of cells of the same volume and number of cells but a spatially uniform cell density (Fig. 5). The cells lining each idealized cylinder experience a constant flux of $F' = rI/2d$ according to the logic in Eq. (3). The cells in the random-layer experience an intensity that decays exponentially with depth according to Eq. (11). In our simple productivity model, cells that experience an irradiance less than the compensation level, or

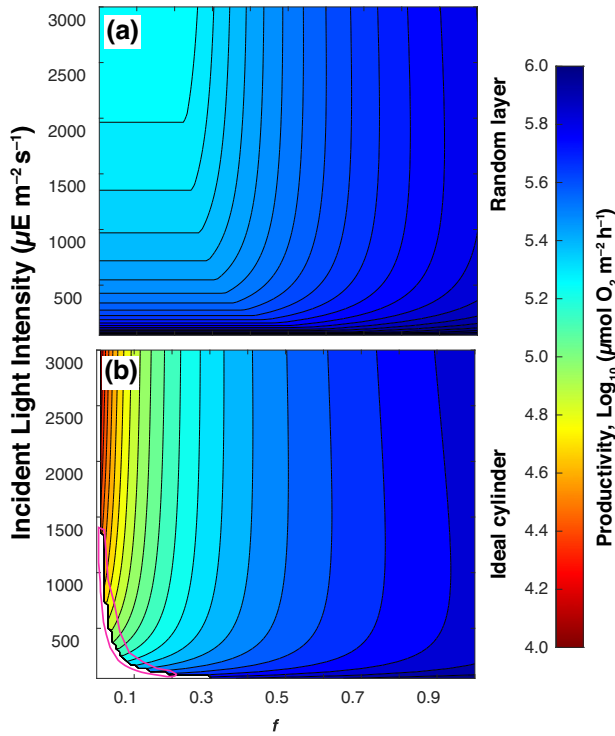


FIG. 5. (a) The calculated productivity of a random layer of algae. (b) The calculated productivity of the simple-cylinder model as a function of the cylinder parameter f and the equivalent average density as the layers represented in (a). The magenta curve indicates the contour of optimal productivity as a function of the intensity and f .

the flux at which the rate of photosynthesis is equal to the rate of cellular respiration, have a productivity of zero. We have assigned the compensation level of *Symbiodinium* to be $15 \mu\text{E m}^{-2} \text{s}^{-1}$ given reports in the literature [27].

In this f - I space, both the random layer and its corresponding cylinder trace out curves that reflect the photosynthesis-irradiance behavior of the underlying system (Fig. 5). The productivity of the cylindrical system sharply increases as f decreases from 0.2 to zero, while the random layer is flat for the same values of f . At the maximum considered incident flux, $I = 3000 \mu\text{E m}^{-2} \text{s}^{-1}$, the productivity of the cylinder was maximum at $f = 0.005$, with a value of $0.9 \text{ mol O}_2 \text{ m}^{-2} \text{h}^{-1}$. At smaller values of f or I , the cylindrical system sees a flux lower than the defined compensation level, such that productivity is zero, indicated by the white region of the plot. In contrast, the comparable random layer has a productivity of $0.06 \text{ mol O}_2 \text{ m}^{-2} \text{h}^{-1}$. In the larger f - I space, the productivity of the random layer has a similar structure to that of the cylinders but has much smaller values of productivity throughout most of the space. When considering the ratio of productivity of the idealized cylindrical system to that of a similar random layer, the cylinders are up to 12 times more productive with the same number of cells in the same volume (Fig. 6). In the upper-right regions of the f - I

space, where intensities are high and cylinders are wider, a random layer is more productive than the cylinder. This is because all the cells in the cylinder are experiencing high photoinhibition, while the exponential attenuation within the random layer ensures that some cells in the layer are operating efficiently.

B. Absolute performance of the system relative to eight photons per molecule of O_2

We have evaluated the light-use efficiency of this model relative to the solar resource using the basic energetic requirement that eight photons of photosynthetically active radiation are required to fix one molecule of O_2 [3]. In the random-layer system, the efficiency relative to the resource decreases as the intensity increases at all values of f . The resource efficiency of the cylinders increases with decreasing f at all intensities, until the point at which further decreases in f drop the system below the compensation level (Fig. 7). The simple-cylinder system can operate close to 70% of perfect resource efficiency at any realistic incident-light intensity. Larger values of f have maximum efficiency at lower incident intensities (e.g., $f = 0.1$ results in 70% efficiency at $250 \mu\text{E m}^{-2} \text{s}^{-1}$) and smaller values of f are more efficient at higher intensities (e.g., $f = 0.05$ is 70% efficient close to $3000 \mu\text{E m}^{-2} \text{s}^{-1}$).

C. Diurnal model of productivity

The overall productivity of any given cylinder or layer depends both on the efficiency associated with a given intensity and on the number of cells experiencing light intensities greater than the cellular compensation level, in our study chosen to be $15 \mu\text{E m}^{-2} \text{s}^{-1}$. So, for any given value of f , cells in the system will exist above or below the compensation level at different times of day. Understanding the absolute performance of our model in natural illumination therefore requires integrating productivity over the natural changes of light intensity over an average day.

To study the performance of our cylinder and layer systems over light intensities changing in time, we have developed a simple model of irradiance over a day in the giant-clam habitat (1-m water depth near the equator). Briefly, we have fitted a Gaussian function to a month-long set of down-welling PAR obtained from a publicly available data set from a weather station in Koror, Palau ([28], Fig. 8). We have then calculated the integrated productivity of our model cylinders and layers over the light-intensity fluctuations characteristic of a 24-h period.

When shifts in incident intensity over a day were incorporated into our productivity calculation, productivity increased with decreasing f , to a value of $2 \text{ mol O}_2 \text{ m}^{-2} \text{day}^{-1}$, which is 42% of the perfectly efficient per-day rate.

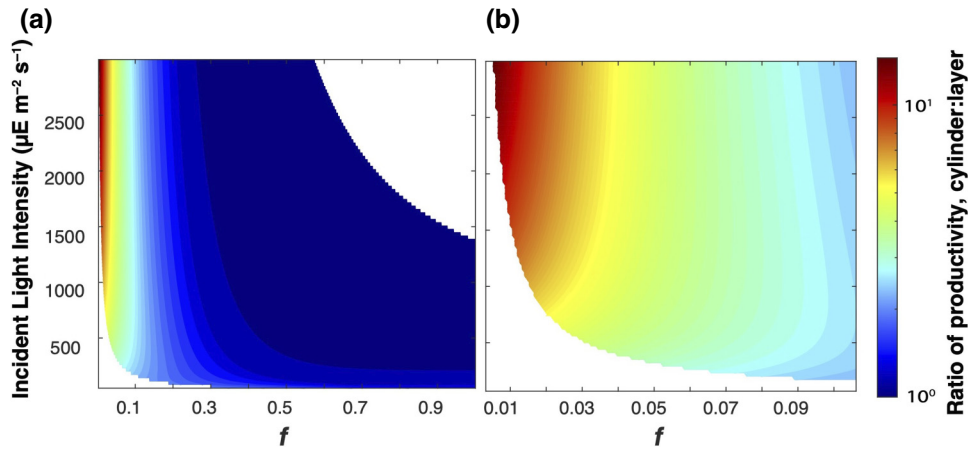


FIG. 6. The ratio of the productivity of a model cylinder to that of an idealized layer in the f - I plane: (a) $0 < f < 1$; (b) $0 < f < 0.1$.

There are, of course, additional complexities in the fluctuations of environmental light experienced by wild clams. Individual clams live at different average depths and experience different tidal fluctuations depending both on geographic location and the lunar cycle. The net productivity of any of these systems will, of course, decrease with decreasing average light intensity in the given ecological niche. Our calculation of the productivity of the system

time averaged over a 24-h period near the surface of the water represents the maximum productivity of a static system in natural sunlight. Clams are frequently immediately under the water surface at low tide, so our calculation does capture an important aspect of the natural history of the real clams. We are interested in the realistic limits of photosynthesis under intense natural sunlight, so this is also the quantity of most interest to our study. However, the performance of any given clamlike system under a different regime of natural variation in illumination can be estimated by inspection of a vertical contour of productivity with the range of light intensities of interest at a given value of f in Fig. 5.

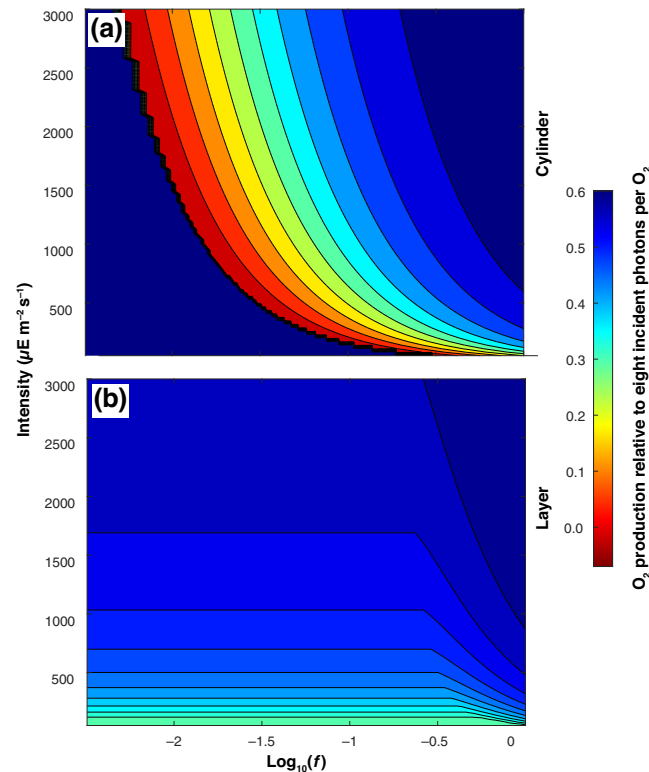


FIG. 7. The absolute efficiency of the cylinder and the random layer. (a) The absolute efficiency of the cylinder model, $\log f$ scale. (b) The absolute efficiency of the random-layer model, $\log f$ scale.

IV. REANALYSIS OF CLASSIC GIANT-CLAM DATA

We have then reanalyzed data from a study published in 1985 by Fisher, Fitt, and Trench [11]. The authors have measured photosynthesis-irradiance behavior of clams of different size and age classes and of algae that were freshly isolated from clams. The data as reported in this paper are shown in Fig. 9.

The original photosynthesis-irradiance data were reported both normalized by the total mass of chlorophyll a in the tissue and by the weight of the clam tissue (Figs. 9(a) and 9(b)). The authors have also reported shell lengths for each individual, which we call ℓ . With this information, we can estimate the horizontally projected surface area of the clam tissue and thereby estimate the solar resource available to the clam. We put a lower bound on the horizontally projected area of the mantle tissue by considering it an ellipse that is half as wide as ℓ . We set an upper bound of the horizontally projected area as a circle with diameter of ℓ , which is certainly an overestimate given the general shape of the clams.

In Fig. 9(c), we show the area-normalized photosynthesis-irradiance relation, with the lower-bound area

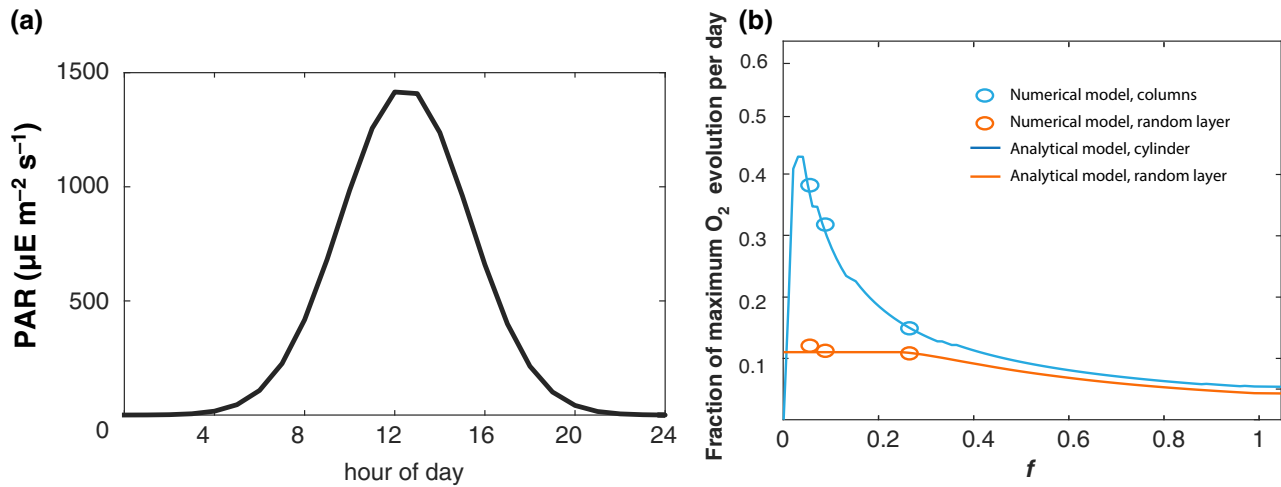


FIG. 8. (a) The model of the daily photosynthetically active radiation experienced by the clams. (b) The system efficiencies when integrated over a day of radiance as shown in (a). The curves show calculations for the analytical models discussed in the text. The circles show equivalent calculations for our numerical model of radiative transfer through a system made of discrete cells. The circles representing the efficiency of the numerical model are placed along the x axis at the point where they are equal to the analytical calculation.

in solid lines and the upper-bound area in dashed lines. We have calculated the per-day resource efficiency as applied above to our cylinder and layer models. The resource efficiency increases roughly linearly with the clam shell length. For the largest clam, the upper and lower bounds of the estimated horizontal area projection result in a resource efficiency of 60% with the large-area bound and 117% with the small-area bound [Fig. 9(d)]. (To be clear, we are not claiming that the clams can possibly have efficiency greater than 100%, just that there is uncertainty around the horizontally projected area of the system.)

For any realistic estimate of the projected horizontal area, the largest clam performs better throughout a day than is possible using any single value of f in our simple-cylinder model (Fig. 7). However, this performance of greater than 60% is possible if a system is able to follow a contour of maximum productivity in f - I space [shown in magenta in Fig. 7(b)]. Remarkably, there is some evidence that clams actually have a behavior that could do this. Clams are able to use blood pressure to inflate and deflate their mantle tissue. If the distance columns of algae within the clam were to increase and decrease with mantle inflation, the clam would be able to modulate the effective value of r , and therefore f , of its array of pillars with daily changes in irradiance.

V. PERFORMANCE WITH MODULATION OF f VIA INFLATION OF THE MANTLE TISSUE

Given that large living clams easily outperform the simple-cylinder model for any fixed value of f over a day,

we have calculated the productivity of the cylinder model such that values of r shift with changes in light intensity (which is potentially realized by the clam when it inflates and deflates its mantle tissue). We have moved this system through a contour of optimum f for a given irradiance value during the day (this contour is circled in magenta in Fig. 5). In this calculation, where f was allowed to be optimal for each incident-light intensity, the cylinder model achieved a resource efficiency of 67%, which is within the predicted range of values for the living clam, given uncertainty about the projected horizontal area, but closer to the minimum bound of 60% for the experimental data.

We have some observational evidence suggesting that clams are indeed able to modulate the effective r of their arrays of columns via inflating and deflating the mantle tissue. We have been able to visualize the locations of algal columns in active living clam tissue by using a bright light-emitting diode with a 450-nm emission and a 700-nm long-pass filter on a digital single-lens reflex camera with a macro lens. We have observed that when the clam tissue inflates, the columns of algae in the tissue get farther apart. The column nearest-neighbor distance increases by around 50% in the mantle movement shown in Fig. 10. Changes in our model parameter f go linearly with the nearest-neighbor distance, which roughly maps to r in the cylinder model. In this experiment, the clam was relaxing and re-inflating from being “startled” but it is at least plausible that similar contraction and inflation behavior happens much more slowly over the course of a day. The optimal performance of the model over the range of usual daylight intensities requires a modulation of f and therefore r of roughly tenfold (Fig. 5). Given the subtlety of

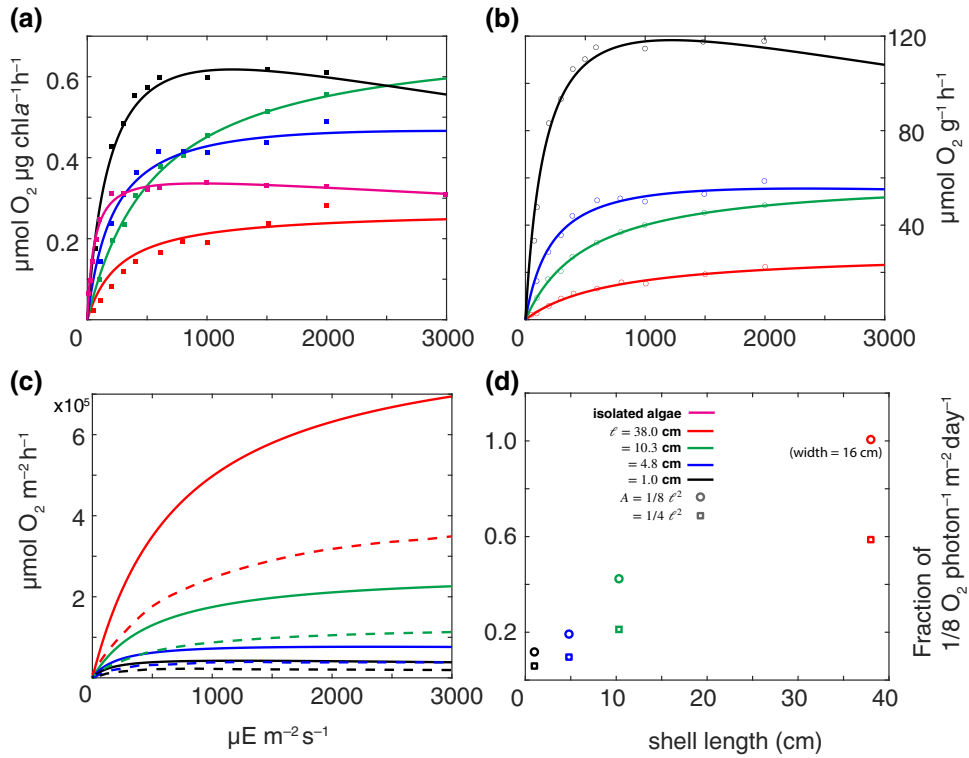


FIG. 9. The original and reanalyzed data from Fisher *et al.* (a) The original photosynthesis-irradiance data for giant clams normalized by chlorophyll *a* content. The symbols show original data points and the curve shows the fit to Eq. (9). (b) The original photosynthesis-irradiance data for the same four clams, normalized by the clam wet weight. The symbols show original data points and the curve shows the fit to Eq. (9). (c) Data from the upper-left panel, renormalized by the estimated mantle area. The solid lines represent the area-normalized PI curve for a clam with a mantle area estimated to be that of an ellipse half as wide as the shell length, ℓ . The dashed lines represent the area-normalized PI curve for a clam with a mantle area equal to a circle with diameter equal to ℓ . (d) The calculation of the per-day solar-resource efficiency of living clams, calculated as described above using PI curves from the lower-left panel, as a function of the shell length for the two different mantle-area estimates in the lower-left panel. The estimate for the largest clam exceeds 100% at the lower-bound estimate of the mantle size; for this point, we assume the mantle width required for efficiency to be 100% of 16 cm = 0.43ℓ .

the movement we observe here that results in a 1.5-fold shift in r , it is at least plausible that the combined effects of inflation of the mantle, rotation of the mantle around the shell, and modulation of the shell opening could modulate the effective r of the clam system through a similar range.

VI. PERFORMANCE OF NUMERICAL MODEL WITH MULTIPLE SCATTERING

The cylinder model incorporating shifts in r and therefore f with the light intensity is able to capture the experimentally observed high resource efficiency of living clams, upward of 60%. The remaining energetic limitation of this model is that it only allows for a single pass of radiation. Light transmitted through the layer of single cells in the cylinder model is by definition rejected by the system. When the cylinders are operating at an efficient light level, the system operates very close to the compensation level and single cells absorb 82% of incident light. Therefore,

any cells in a shadow of the direct incoming beam must receive multiple-scattering events from seven or eight other cells to also be above the compensation level and contribute to the production of the larger system. While this is physically possible, locating any geometric solution that achieves this for all cells in the system is nontrivial. However, the loosely packed columns of cells observed in the real clam system may allow for this additional source of resource-level efficiency via multiple scattering to occur.

To investigate the possible effect of multiple scattering within the clam tissue, we have reutilized a Monte Carlo model of radiative transfer through a system of clamlike iridocytes and algae with discrete positions, the method for which is documented in Ref. [19]. Briefly, a thin layer of cells that have the optical phase function of iridocytes is present at the surface of the system; underneath the iridocytes are columnar arrays of algae, the densities of which within the columns and the column lengths of which approximate the clam system as closely as possible. For

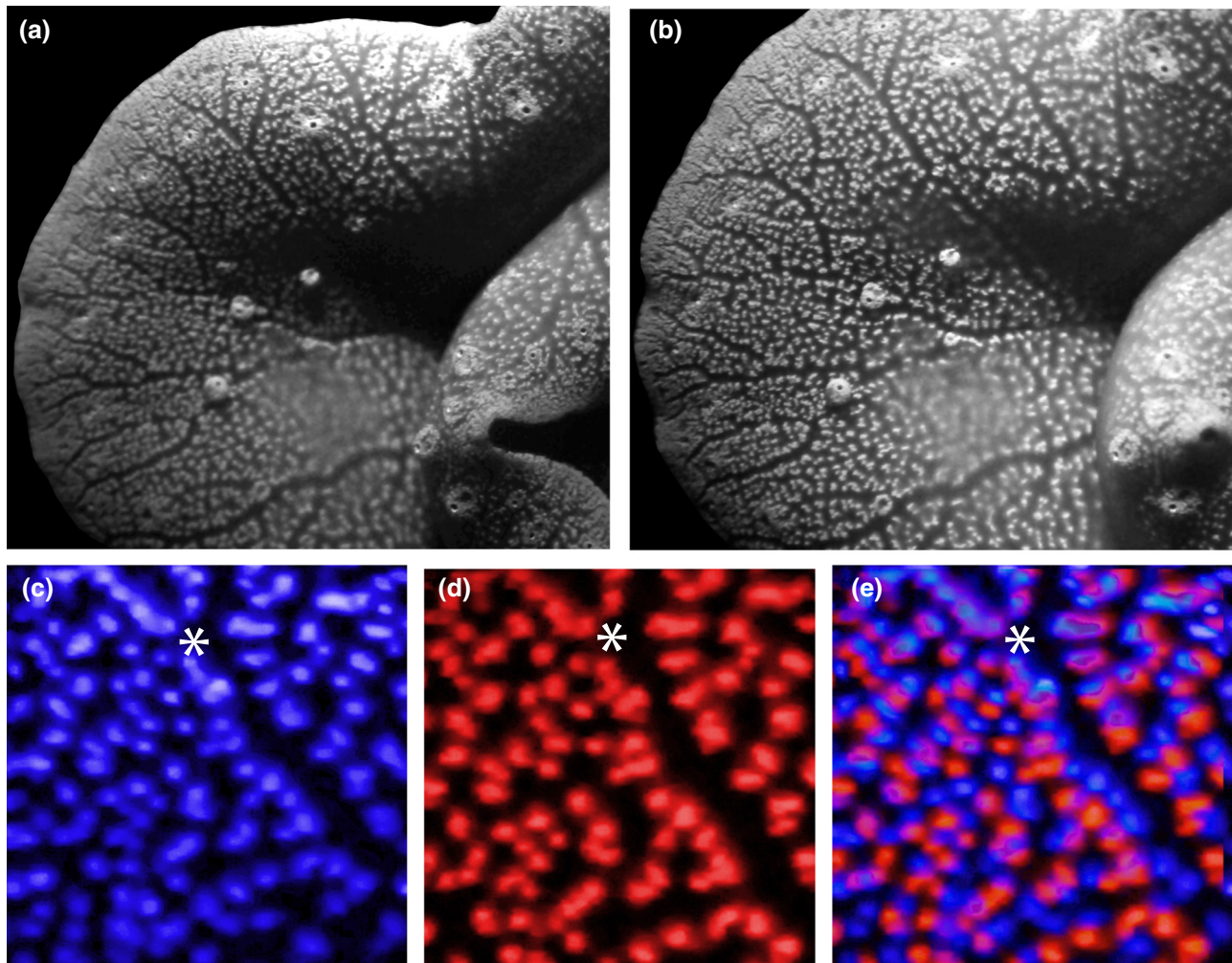


FIG. 10. The inflation and stretching of relative column locations. (a) The living clam mantle in an initial configuration imaged using chlorophyll fluorescence, with the columns relatively close together. (b) The same living clam mantle 1 min later, with the mantle inflated by blood pressure and the algal columns farther apart. (c) A false-color image of a subregion in (a). (d) A false-color image of the same subregion in (b). (e) An overlay of (c) and (d). The asterisks show the point at which the images from (a) and (b) are aligned. The columns in (d) (red) are stretched in position relative to the same columns in (c) (blue) approximately 1 min earlier in time.

this study, we have used cell coordinates for which the cell and chlorophyll a densities matched the individual clams the PI curves of which were measured experimentally in Fisher *et al.* [11] as closely as possible given the information available [Figs. 11(a)–11(d)]. We have fixed the column locations to the positions used in Ref. [19] but increased the length of the pillars relative to the work in Ref. [19] as in order to account for the data reported for algal density as a function of clam shell length in [11], thereby ensuring the areal density of algae matches that of the clams in that study. The ultimate effect of making the columns longer in the larger clams is to decrease the effective f as the clams grow. We have then also compared these results for realistic clam tissue to those of a randomly organized layer with the same cell number, analogous to the analytical model described above.

The results of this numerical model of radiative transfer recapitulate those from the static simple-cylinder models surprisingly well, with the smallest system with the largest effective f achieving 17% resource efficiency, the system with intermediate f achieving 32% resource efficiency, and the largest system, meant to model the largest clam from in the Trench study, achieving 39% of the resource efficiency (Fig. 8).

In the radiative transfer model, the algae within the columnar structures are organized randomly and at a density such that the whole-tissue average of the cell density matches that of experimental observation. This random organization does not result in any efficiency gains over the single-pass simple cylinders with fixed f described above. Therefore, it seems that the primary way in which the clam achieves efficiencies greater than the

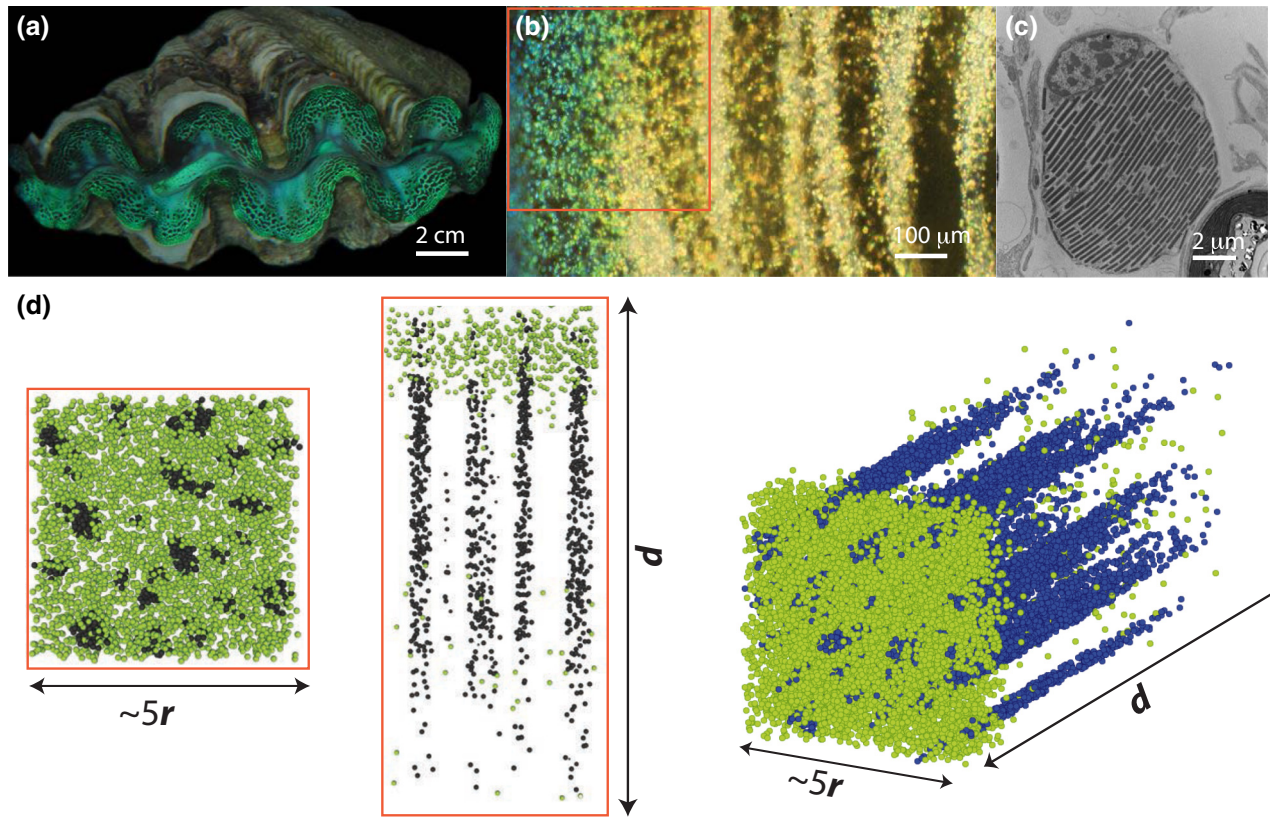


FIG. 11. A numerical Monte Carlo model of multiple scattering within clam tissue and its relation to the living clam. (a) A small living clam, showing the general appearance and relation between the shell length and the width of the exposed mantle tissue. (b) A low-magnification micrograph showing dark regions of algae under a thin array of iridocyte cells. (c) A transmission electron micrograph of a single clam iridocyte. (d) The specific cell coordinates of our Monte Carlo model of detailed multiple scattering within the clam tissue. Single-celled *Symbiodinium* are shown in blue and iridocytes are shown in green.

fixed- f cylinder model is through inflating and deflating the tissue and thereby modulating f with the intensity of the first-pass light in the system. Any additional efficiency gains achieved through multiple light scattering inside a column evidently require a nontrivial organization of cells within a column. Specifically, all cells in the interior of a column must be positioned such that they receive light forward scattered from about eight other cells simultaneously in order to be above the light level at which photosynthesis exceeds cellular respiration (i.e., in our model, the compensation level of $15 \mu\text{E m}^{-2} \text{s}^{-1}$ defined above). We speculate that if living cells are able to migrate to optimum locations to intercept light in the interior of a column, either through attrition or active movement, the clam system may be able to realize efficiency gains through optimum absorbance of multiply scattered light. Given the uncertainty around estimating the projected horizontal area of the clam, it is uncertain whether this additional mechanism is required to fully explain the efficiencies observed in the living clam by Fisher and colleagues [11]. Additional investigation will be required to understand this aspect of the system.

VII. SCALE INVARIANCE OF THE SYSTEM

Our study has initially been inspired by our observations of giant clams but the principles we outline are generalizable to photosynthetic systems at any spatial scale; the photosynthetic performance of our model ultimately depends on a ratio of lengths, so the model could in principle operate at any length scale. In considering the possible scale invariance of our model, we have observed that aerial photographs of coniferous trees in boreal forests strongly resemble micrographs of the vertical columns found within the clam skin, particularly if the scale of the images is not known (Fig. 12).

We conjecture that in forests, individual spruce trees could perform the structural and optical role of individual columns of algae in the clam system but at a much greater length scale. For this to be true, the conifer forest would also require a light-scattering element with a similar phase function, or angular scattering probability, to the iridocytes of the clam. Surprisingly, despite the big differences in size and composition between a layer of clam iridocytes and clouds, the effective phase functions of

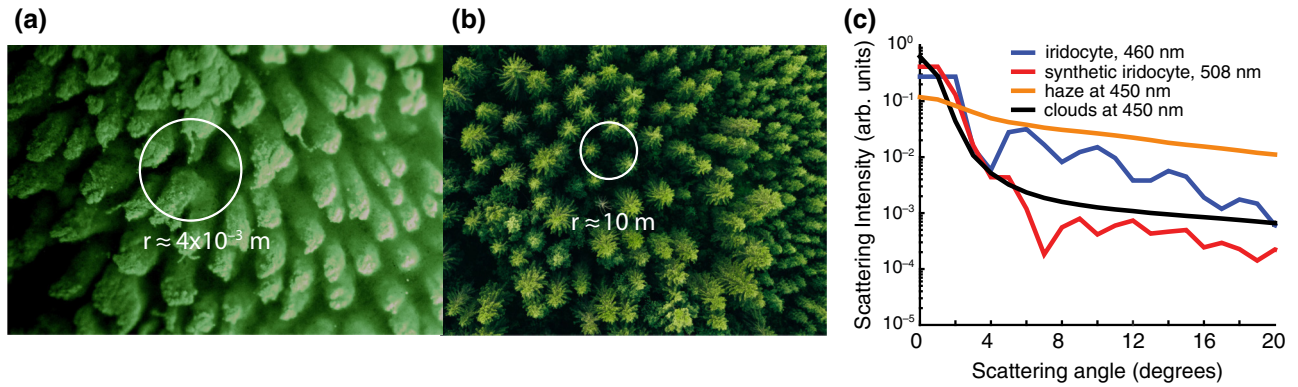


FIG. 12. (a) The column structures within clam tissue at length scales of tens of micrometers, visualized with 450-nm illumination and 750-nm long-pass filtered light. (b) An aerial photograph of spruce trees in boreal forest strongly resembles the columnar structures in the clam at a different length scale. (c) A comparison of the scattering behavior of clams iridocytes (blue curve) and clouds and haze (yellow and black curves). Image in (b) via CanStockPhoto at a location near the BOREAS long-term study site “NSA-UBS” at coordinates (55.908° N, -51.519° W); data in (c) from Refs. [20,29].

clouds and fog are remarkably similar to the phase functions of the clam iridocytes (see Fig. 12; see also Refs. [29,30]). To rationalize this possible similarity between the two systems, we have considered the mean free path or average number of scattering events within a layer of clouds and within a layer of iridocytes. Our prior characterization of clam tissue in Ref. [19] shows that a layer of iridocytes is about $300 \mu\text{m}$ thick, with a density of $9.3 \times 10^7 \text{ cells cm}^{-3}$ resulting in around 1.43 scattering events as light traverses the layer. In comparison, average cloud cover over a conifer forest is about 300 m thick with around $100 \text{ particles cm}^{-3}$, similarly resulting in around 1.5 scattering events as light traverses the cloud [29,30].

Therefore, we predict that clouds over spruce forest perform the same optical role as iridocytes in the clam system (Fig. 12(c); see also Refs. [27,29]). If spruce forests do exhibit high light-use efficiencies with a physical mechanism similar to that of giant clams, we would predict that the albedo of these forests would be lower than that of other kinds of forest. Both clams and spruce forests have unusually low albedo for large photosynthesizing systems; we have observed that clam albedo is as low as 5% and mature conifer forests have a similar albedo of around 7% [31]. In comparison, the albedo of Amazon forest is around 12% and that of soybean crops is around 17% [32,33]. Our model also predicts that mature conifer forests with tall and regularly spaced trees will exhibit greater light-use efficiency under cloudy conditions (when the phase function of down-welling light results in a more even distribution along the vertical aspect of the trees, as in the clam), independent of the overall light intensity. Indeed, this seems to be the case. In a broad survey of the light-use efficiency of Canadian biomes, the most mature homogeneous conifer forests, which are most like our clam-inspired model, exhibited the strongest positive relationship between the fraction of diffuse radiation and

the light-use efficiency of any boreal vegetation type considered [34]. Interestingly, this study also calculated light-use efficiencies occasionally exceeding 100% based on the same efficiency definition of eight photons per O_2 that we have used here when the conditions were most diffuse [34]. Spruce trees presumably cannot rapidly modulate intertree spacing as a function of daily light fluctuations, as we predict to be the case for clams. However, even a static system that operates according to our simple-cylinder model (such as a spruce forest) will still exhibit several-fold higher efficiency with respect to the solar resource than the same system when randomly organized (as may be closer to the case for broadleaf-dominated forests) (Fig. 6; see also Ref. [35]).

VIII. CONCLUSIONS

Inspired by photosymbiotic giant clams, we have developed an analytical model of photosynthetic performance that explains how a clamlike geometry can extend much of the high efficiencies at the small scales of single photosystems to up to the large length scales of organisms and ecosystems. Our model defines a light-dilution factor or f , describing the geometry of the constituent cylinders of absorbers in the system, that should optimally change with the incident-light intensity. In such a system that can modulate f with environmental intensity changes, a light-use efficiency with respect to the solar resource of 67% can be achieved under the daily fluctuations in light intensity characteristic of shallow water in the tropics. Surprisingly, this idealized efficiency from our analysis is near the minimum-bound efficiency estimated from a photosynthesis-irradiance experiment on living giant clams in 1985 [11]. This result suggests that the animals must actively modulate the effective value of f of the photosynthetic tissue by inflating and deflating the tissue

around the clam shell (Fig. 10). Further efficiency gains allowing the animal to approach a near-perfect conversion of light into oxygen, as suggested by the experimental data, could come from optimizing the interception of multiply scattered light in the interior of the algal columns of the tissue. Our numerical model that captures multiple scattering within columns containing randomly organized algae exhibits roughly the same efficiency as the simpler analytical model, suggesting that such a solution, while physically allowed, is nontrivial to locate. A solution that optimizes multiple scattering therefore evidently requires nontrivial positioning or migration of algae inside the columns. Our simple model assumes that collimated downwelling light is scattered along the vertical aspects of the cylinders in a perfectly even manner. In clams, iridocytes perform this function and for an engineered system of consisting of algae, an environmentally benign and straightforward procedure involving silica microparticles has been described that accomplishes very similar light-scattering behavior [20]. Remarkably, clouds and haze may perform the same scattering role at the scale of tens of meters in similarly efficient boreal forests.

Our study inspired by the clam system also provides an important fundamental insight into the related problem of utilizing contemporary (as opposed to fossil) biomass as an energy source. The analytical model presented here will readily generalize to any photosynthetic system made of living cells or photolabile material with homogeneous vertical light distribution, i.e., light dilution. Therefore, it provides a strategy to optimize light-use efficiency for any photosynthetic cell type or photolabile photovoltaic material under any constant or fluctuating light regime. For the particular cells and the apparent ability to modulate geometry with light intensity found in the clam system, we find a maximum light-use efficiency of 67% by following a contour of maximum efficiency with light and intensity found in our model. Further dilution of the light with an increasing cylinder aspect ratio places individual cells below the compensation level at which respiration exceeds photosynthesis, lessening the overall production and efficiency of the system. So, this exact result of 67% is specific to the giant clams and the strain of *Symbiodinium* isolated from them by Fisher and colleagues [11] and the constituent photosynthesis-irradiance behavior characterized there; maximum efficiencies of different systems with similar geometries and light-scattering properties will differ slightly with a given photosynthetic cell type and its characteristic photosynthesis-irradiance behavior. However, we note that these are all properties that are readily amenable to further modeling and engineering. A study calculating the physical upper limit of algal biofuel cultivation has estimated that under realistic tropical solar radiation, an alga that produces 70% of its dry weight as oil could generate around 60 000 l per hectare per year of liquid fuel [36]. This calculation assumes a 50% photon

utilization efficiency from the algae. The clams appear to meet all the assumptions of this calculation about the rest of the energy-transduction pathway from the sun to photosynthate and our work suggests that large clams exceed the estimated realistic maximum photon-utilization efficiency in that work [36]. So, a large system that follows the physical principles that we have outlined for the clam could in principle exceed a productivity of 60 000 l per hectare per year of fuel. Therefore, we anticipate our model to be a useful tool in designing future schemes for efficient photosynthetic biomass cultivation. It may be particularly useful in designing schemes for optimally efficient production of algal biofuels and in conceptualizing minimum land-use requirements for sustainable biomass harvesting for any arbitrary photosynthetic or organic photovoltaic system in the future.

All numerical calculations and figures were made using MATLAB and all underlying code is available on request from the authors.

ACKNOWLEDGMENTS

We thank the staff and scientists of the Palau International Coral Reef Center and the Palau Mariculture Display Center for their efforts in giant-clam conservation and their help in working with these animals. This work was funded by a Packard Foundation Fellowship to A.M.S. and by National Science Foundation (NSF) Award No. IOS-1343159. Solar-irradiance data were provided by PacIOOS, which is a part of the U.S. Integrated Ocean Observing System (IOOS[®]), funded in part by National Oceanic and Atmospheric Administration (NOAA) Awards No. NA16NOS0120024 and No. NA21NOS0120091.

- [1] X.-G. Zhu, S. P. Long, and D. R. Ort, Improving photosynthetic efficiency for greater yield, *Annu. Rev. Plant. Biol.* **61**, 235 (2010).
- [2] E. Weis and J. A. Berry, Quantum efficiency of photosystem II in relation to “energy”-dependent quenching of chlorophyll fluorescence, *Biochim. Biophys. Acta-Bioenerg.* **894**, 198 (1987).
- [3] J. R. Bolton and D. O. Hall, The maximum efficiency of photosynthesis, *Photochem. Photobiol.* **53**, 545 (1991).
- [4] C.-Y. Chen, K.-L. Yeh, R. Aisyah, D.-J. Lee, and J.-S. Chang, Cultivation, photobioreactor design and harvesting of microalgae for biodiesel production: A critical review, *Bioresour. Technol.* **102**, 71 (2011).
- [5] P. Kirnev, J. Carvalho, L. Vandenberghe, S. Karp, and C. Soccol, Technological mapping and trends in photobioreactors for the production of microalgae, *World J. Microbiol. Biotechnol.* **36**, 42 (2020).
- [6] C. Posten, Design principles of photo-bioreactors for cultivation of microalgae, *Eng. Life. Sci.* **9**, 165 (2009).
- [7] J. Legrand, A. Artu, and J. Pruvost, A review on photobioreactor design and modelling for microalgae production, *React. Chem. Eng.* **6**, 1134 (2021).

- [8] D. Simionato, S. Basso, G. M. Giacometti, and T. Morosinotto, Optimization of light use efficiency for bio-fuel production in algae, *Biophys. Chem.* **182**, 71 (2013).
- [9] E. G. Nwoba, D. A. Parlevliet, D. W. Laird, K. Alameh, and N. R. Moheimani, Light management technologies for increasing algal photobioreactor efficiency, *Algal Res.* **39**, 101433 (2019).
- [10] W. Blanken, M. Cuaresma, R. H. Wijffels, and M. Janssen, Cultivation of microalgae on artificial light comes at a cost, *Algal Res.* **2**, 333 (2013).
- [11] C. R. Fisher, W. K. Fitt, and R. K. Trench, Photosynthesis and respiration in *Tridacna gigas* as a function of irradiance and size, *Biol. Bull.* **169**, 230 (1985).
- [12] D. Klumpp and J. Lucas, Nutritional ecology of the giant clams *Tridacna tevoroa* and *T. derasa* from Tonga: Influence of light on filter-feeding and photosynthesis, *Mar. Ecol. Prog. Ser.* **107**, 147 (1994).
- [13] W. K. Fitt and R. K. Trench, Spawning, development, and acquisition of zooxanthellae by *Tridacna squamosa* (mollusca, bivalvia), *Biol. Bull.* **161**, 213 (1981).
- [14] K. E. Brodersen, M. Lichtenberg, P. J. Ralph, M. Kühl, and D. Wangpraseurt, Radiative energy budget reveals high photosynthetic efficiency in symbiont-bearing corals, *J. R. Soc. Interface* **11**, 20130997 (2014).
- [15] N. Kramer, J. Guan, S. Chen, D. Wangpraseurt, and Y. Loya, Morpho-functional traits of the coral stylophora pistillata enhance light capture for photosynthesis at mesophotic depths, *Commun. Biol.* **5**, 861 (2022).
- [16] E. J. Hochberg, M. J. Atkinson, and S. Andréfouët, Spectral reflectance of coral reef bottom-types worldwide and implications for coral reef remote sensing, *Remote Sens. Environ.* **85**, 159 (2003).
- [17] U. I. O. O. System, Pacific islands ocean observing system (2024), <https://www.pacioos.hawaii.edu/weather/obs-koror/> (accessed on March 20, 2024).
- [18] M. Darecki, D. Stramski, and M. Sokólski, Measurements of high-frequency light fluctuations induced by sea surface waves with an underwater porcupine radiometer system, *J. Geophys. Res.: Oceans* **116**, C00H09 (2011).
- [19] A. L. Holt, S. Vahidinia, Y. L. Gagnon, D. E. Morse, and A. M. Sweeney, Photosymbiotic giant clams are transformers of solar flux, *J. R. Soc. Interface* **11**, 20140678 (2014).
- [20] H.-N. Kim, S. Vahidinia, A. L. Holt, A. M. Sweeney, and S. Yang, Geometric design of scalable forward scatterers for optimally efficient solar transformers, *Adv. Mater.* **29**, 1702922 (2017).
- [21] C. Jantzen, C. Wild, M. El-Zibdah, H. A. Roa-Quiaoit, C. Haacke, and C. Richter, Photosynthetic performance of giant clams, *Tridacna maxima* and *T. squamosa*, red sea, *Mar. Biol.* **155**, 211 (2008).
- [22] A. J.-Y. Yau and T.-Y. Fan, Size-dependent photosynthetic performance in the giant clam *Tridacna maxima*, a mixotrophic marine bivalve, *Mar. Biol.* **159**, 65 (2012).
- [23] C. Liu, X. Li, C. Wu, A. Wang, and Z. Gu, Effects of three light intensities on the survival, growth performance and biochemical composition of two size giant clams *Tridacna crocea* in the Southern China Sea, *Aquaculture* **528**, 735548 (2020).
- [24] D. Klumpp, B. Bayne, and A. Hawkins, Nutrition of the giant clam *Tridacna gigas* (L.) I. Contribution of filter feeding and photosynthates to respiration and growth, *J. Exp. Mar. Biol. Ecol.* **155**, 105 (1992).
- [25] P. Eilers and J. Peeters, A model for the relationship between light intensity and the rate of photosynthesis in phytoplankton, *Ecol. Modell.* **42**, 199 (1988).
- [26] S. Enríquez, E. R. Méndez, and R. I. Prieto, Multiple scattering on coral skeletons enhances light absorption by symbiotic algae, *Limnol. Oceanogr.* **50**, 1025 (2005).
- [27] S. Karako-Lampert, D. Katcoff, Y. Achituv, Z. Dubinsky, and N. Stambler, Responses of *Symbiodinium microadriaticum* clade B to different environmental conditions, *J. Exp. Mar. Biol. Ecol.* **318**, 11 (2005).
- [28] <https://www.pacioos.hawaii.edu/weather/obs-koror/>
- [29] J. E. Hansen, Exact and approximate solutions for multiple scattering by cloudy and hazy planetary atmospheres, *J. Atmos. Sci.* **26**, 478 (1969).
- [30] D. Deirmendjian, Scattering and polarization properties of water clouds and hazes in the visible and infrared, *Appl. Opt.* **3**, 187 (1964).
- [31] A. K. Betts and J. H. Ball, Albedo over the boreal forest, *J. Geophys. Res.: Atmos.* **102**, 28901 (1997).
- [32] A. Culf, G. Fisch, and M. Hodnett, The albedo of Amazonian forest and ranch land, *J. Clim.* **8**, 1544 (1995).
- [33] M. H. Costa, S. N. Yanagi, P. J. Souza, A. Ribeiro, and E. J. Rocha, Climate change in Amazonia caused by soybean cropland expansion, as compared to caused by pastureland expansion, *Geophys. Res. Lett.* **34** (2007).
- [34] C. R. Schwalm, T. A. Black, B. D. Amiro, M. A. Arain, A. G. Barr, C. P.-A. Bourque, A. L. Dunn, L. B. Flanagan, M.-A. Giasson, and P. M. Lafleur, *et al.*, Photosynthetic light use efficiency of three biomes across an east-west continental-scale transect in Canada, *Agric. For. Meteorol.* **140**, 269 (2006).
- [35] D. D. Baldocchi and C. A. Vogel, Energy and CO₂ flux densities above and below a temperate broad-leaved forest and a boreal pine forest, *Tree Physiol.* **16**, 5 (1996).
- [36] K. M. Weyer, D. R. Bush, A. Darzins, and B. D. Willson, Theoretical maximum algal oil production, *Bioenergy Res.* **3**, 204 (2010).